MRSA

Restoring Methicillin-Resistant *Staphylococcus aureus* Susceptibility to β-Lactam Antibiotics

Christopher M. Tan,[1]* Alex G. Therien,[1]* Jun Lu,[2] Sang H. Lee,[1] Alexandre Caron,[3] Charles J. Gill,[1] Christian Lebeau-Jacob,[3] Liliana Benton-Perdomo,[3] João M. Monteiro,[4] Pedro M. Pereira,[4] Nathaniel L. Elsen,[5] Jin Wu,[1] Kathleen Deschamps,[1] Mihai Petcu,[3] Simon Wong,[3] Etienne Daigneault,[3] Susanne Kramer,[1] Lianzhu Liang,[1] Eugene Maxwell,[1] David Claveau,[3] John Vaillancourt,[3] Kathryn Skorey,[3] John Tam,[3] Hao Wang,[1] Timothy C. Meredith,[3] Susan Sillaots,[3] Lisa Wang-Jarantow,[1] Yeeman Ramtohul,[3] Eric Langlois,[3] France Landry,[3] John C. Reid,[2] Gopal Parthasarathy,[2] Sujata Sharma,[5] Anastasia Baryshnikova,[6] Kevin J. Lumb,[5] Mariana G. Pinho,[4] Stephen M. Soisson,[2] Terry Roemer[1†]

Despite the need for new antibiotics to treat drug-resistant bacteria, current clinical combinations are largely restricted to β-lactam antibiotics paired with β-lactamase inhibitors. We have adapted a *Staphylococcus aureus* antisense knockdown strategy to genetically identify the cell division Z ring components—FtsA, FtsZ, and FtsW—as β-lactam susceptibility determinants of methicillin-resistant *S. aureus* (MRSA). We demonstrate that the FtsZ-specific inhibitor PC190723 acts synergistically with β-lactam antibiotics in vitro and in vivo and that this combination is efficacious in a murine model of MRSA infection. Fluorescence microscopy localization studies reveal that synergy between these agents is likely to be elicited by the concomitant delocalization of their cognate drug targets (FtsZ and PBP2) in MRSA treated with PC190723. A 2.0 Å crystal structure of *S. aureus* FtsZ in complex with PC190723 identifies the compound binding site, which corresponds to the predominant location of mutations conferring resistance to PC190723 (PC190723^R). Although structural studies suggested that these drug resistance mutations may be difficult to combat through chemical modification of PC190723, combining PC190723 with the β-lactam antibiotic imipenem markedly reduced the spontaneous frequency of PC190723^R mutants. Multiple MRSA PC190723^R FtsZ mutants also displayed attenuated virulence and restored susceptibility to β-lactam antibiotics in vitro and in a mouse model of imipenem efficacy. Collectively, these data support a target-based approach to rationally develop synergistic combination agents that mitigate drug resistance and effectively treat MRSA infections.

INTRODUCTION

Beginning with the discovery of penicillin, β-lactam antibiotics and their more potent and broad-spectrum derivatives (for example, cephalosporins and carbapenems) have markedly improved human health and remain the most heavily used class of antibiotics (*1*). Drug resistance within this class, however, continues to emerge (*2*), and regardless of improvements made in their activity (*3*, *4*), resistance has appeared as early as 1 year after their approval for clinical use (*5*). Augmenting β-lactam antibiotics with a second agent that inhibits β-lactamases—enzymes that hydrolyze the β-lactam core and are the predominant determinant of clinical resistance among Gram-negative bacterial pathogens—has proven a highly effective combination therapy to treat otherwise drug-resistant bacteria (*6*). However, β-lactamases are not the predominant mechanism of β-lactam resistance among Gram-positive bacterial pathogens, including epidemic strains of methicillin-resistant *Staphylococcus aureus* (MRSA) (*2*), which has been estimated to account for mortality rates exceeding that of HIV/AIDS in the United States (*7*). Thus, strategies analogous to those implemented for Gram-negative pathogens are required to restore the efficacy of β-lactam antibiotics against Gram-positive pathogens such as MRSA.

MRSA becomes resistant to β-lactam antibiotics by acquiring the *mecA* gene, which encodes an additional penicillin-binding protein (PBP2A) that blocks β-lactam antibiotic action (*5*, *8*–*12*). Despite significant efforts to design new β-lactam antibiotics that can overcome PBP2A, success has been limited (*3*, *4*, *13*). As an alternative strategy, we sought to identify new targets involved in essential cellular processes whose genetic modulation by even partial inactivation would abrogate MRSA resistance to β-lactam antibiotics. Small-molecule inhibitors to such targets are predicted to display synergistic activity in combination with β-lactams. Further, target-based resistance to such agents by mutations that even mildly compromise protein function are predicted to recapitulate the β-lactam hypersusceptibility phenotype originally demonstrated by subtle antisense-mediated depletion of the target. Such "potentiation" targets of β-lactam antibiotic action would therefore be highly desirable from the perspective of mitigating drug resistance and would provide a rational basis for developing effective new antibiotic combination agents.

RESULTS

Cell division β-lactam susceptibility determinants of MRSA

We adapted an antisense-based genetic knockdown strategy to conditionally repress gene expression in the MRSA COL strain of *S. aureus*

[1]Infectious Diseases, Merck Research Laboratories, Kenilworth, NJ 07033, USA. [2]Global Structural Chemistry, Merck Research Laboratories, West Point, PA 19486, USA. [3]Merck Frosst Canada, Kirkland, Quebec H9H 3L1, Canada. [4]Instituto de Tecnologia Química e Biológica, Universidade Nova de Lisboa, 2781-901 Oeiras, Portugal. [5]Screening and Protein Science, Merck Research Laboratories, West Point, PA 19486, USA. [6]Department of Molecular Genetics, University of Toronto, Toronto, Ontario M5S 3E1, Canada.
*These authors contributed equally to this work.
†To whom correspondence should be addressed. E-mail: terry_roemer@merck.com

(*14*, *15*). We first performed a phenotypic screen for restored β-lactam susceptibility among 245 essential genes in two clinically relevant MRSA strains (*16*). A chemical genetic interaction network is shown summarizing those genes that, under partially repressing conditions, restore MRSA COL susceptibility to imipenem (a clinically important β-lactam carbapenem class antibiotic developed by Merck), as well as multiple additional β-lactam antibiotics, including piperacillin, ertapenem, ceftriaxone, ceftazidime, and cefepime (Fig. 1A). Consistent with previous findings, most β-lactam susceptibility determinants functionally participate in cell wall peptidoglycan biosynthesis (*glm*, *mur*, *mra*, *fem*, *pbp*, and SAV1754 genes), other aspects of cell wall biogenesis (*tarL*, *spsB*, and SAV1892), or wall stress signal transduction pathways (SAV1220) (*15*–*18*). An additional group of β-lactam susceptibility determinants included components of the cell division Z ring, an ancestral tubulin-like macromolecular structure required for assembly of the divisome. The divisome coordinates bacterial cytokinetic machinery, cell wall synthesis, cell constriction, and septation (*19*, *20*) (Fig. 1B). These divisome β-lactam susceptibility determinants included the bacterial functional counterpart of mammalian β-tubulin, FtsZ, as well as the FtsZ accessory proteins FtsA and FtsW (*19*, *20*).

FtsZ is a self-activating guanosine triphosphatase (GTPase) that polymerizes into cytoskeletal Z ring filaments that localize to the future division site at the mid-cell early in the cell cycle (*20*). Localization studies reveal that FtsZ lies immediately adjacent to the cytosolic face of the plasma membrane in cells initiating division, forming a ring that constricts during septation (*21*). The Z ring is highly dynamic in structure, and although its mechanical properties are not fully understood, cell cycle–regulated GTPase activity intrinsic to FtsZ may promote bending of FtsZ filaments sufficiently to generate a contractile force around the Z ring (*20*, *22*).

FtsZ and other Z ring components likely serve as β-lactam susceptibility determinants through their functional role in the recruitment of downstream components of the divisome, including proteins required for cell wall peptidoglycan synthesis, such as PBPs, the targets of β-lactam antibiotics (*19*, *23*). Perturbations in Z ring assembly impair cell wall assembly (*24*). Moreover, multiple PBPs are delocalized from the septum by cell wall perturbations (*19*, *25*). PBP2, the target of imipenem, is itself delocalized from the septum in *S. aureus* upon genetic depletion of FtsZ (*26*).

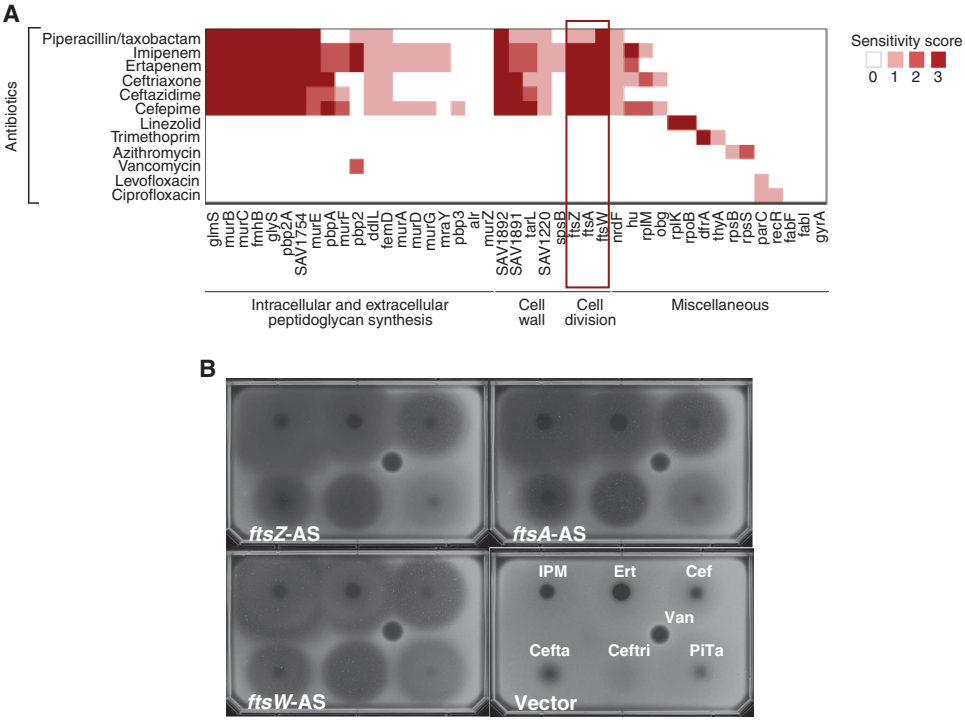

Fig. 1. Chemical-genetic interaction network for imipenem. (**A**) Hypersensitivity phenotypes between antisense-bearing strains of MRSA COL and select antibiotics are summarized in a clustergram display and color-coded according to qualitative scoring of their phenotype (strong, 3; medium, 2; mild, 1; none, 0) (*16*). β-Lactam antibiotics include penicillin, piperacillin (combined with β-lactamase inhibitor tazobactam; PiTa), carbapenems (imipenem, IPM; ertapenem, Ert), and cephalosporins, ceftriaxone (Ceftri), ceftazidime (Cefta), and cefepime (Cef). Clinically relevant non–β-lactam antibiotics include linezolid, trimethoprim, azithromycin, vancomycin (Van), levofloxacin, and ciprofloxacin. (**B**) MRSA COL β-lactam hypersusceptibility phenotypes of *ftsZ*-, *ftsA*-, and *ftsW*-AS–bearing strains under partial antisense induction (plus 50 mM xylose) versus vector control using an agar susceptibility assay. MRSA strains were inoculated in LB agar medium, and the listed antibiotics were spotted identically on the surface of each of the four agar-seeded plates. Dark halos at the position of antibiotic spotting reflect the zone of inhibition (that is, growth inhibition) produced by each antibiotic. Compared to the vector control containing the MRSA COL strain, *ftsZ*, *ftsA*, and *ftsW*-AS strains each display prominent hypersensitivity to each of the β-lactam antibiotics tested. The non–β-lactam antibiotic vancomycin is spotted as a control for the β-lactam hypersusceptibility phenotypes observed for *ftsZ*, *ftsA*, and *ftsW*-AS strains.

Synergistic activity between β-lactam antibiotics and FtsZ inhibitor PC190723

Chemical-genetic interaction networks predict compound synergy between cognate inhibitors of such targets and their corresponding companion antibiotic (*15*, *16*). Accordingly, we tested this hypothesis using the small-molecule PC190723, which is a recently reported inhibitor of *S. aureus* FtsZ (*27*, *28*). Confirming our genetic prediction, PC190723 and imipenem displayed in vitro synergy against MRSA (Fig. 2A). PC190723 has a synergistic inhibitory concentration [SIC, herein defined as the minimum inhibitory concentration (MIC) in the presence of imipenem at 4 μg/ml, which is the clinical breakpoint for this antibiotic against *S. aureus*] of 0.25 to 0.5 μg/ml. PC190723 was also synergistic when combined with all β-lactam antibiotic subclasses tested; synergy was rarely observed when paired with other antibiotic classes (table S1). PC190723-imipenem synergistic activity was further tested across 105 methicillin-sensitive and methicillin-resistant clinical isolates of various *Staphylococcus* species, with PC190723 SIC values of ≤0.25 μg/ml in combination with imipenem (4 μg/ml) against 53 of 59 methicillin-resistant strains examined (table S2). PC190723 also produced strong microbiological activity as a single agent, displaying a lower MIC_{90} (0.5 μg/ml; minimum inhibitor concentration against 90% of clinical strain isolates tested) than

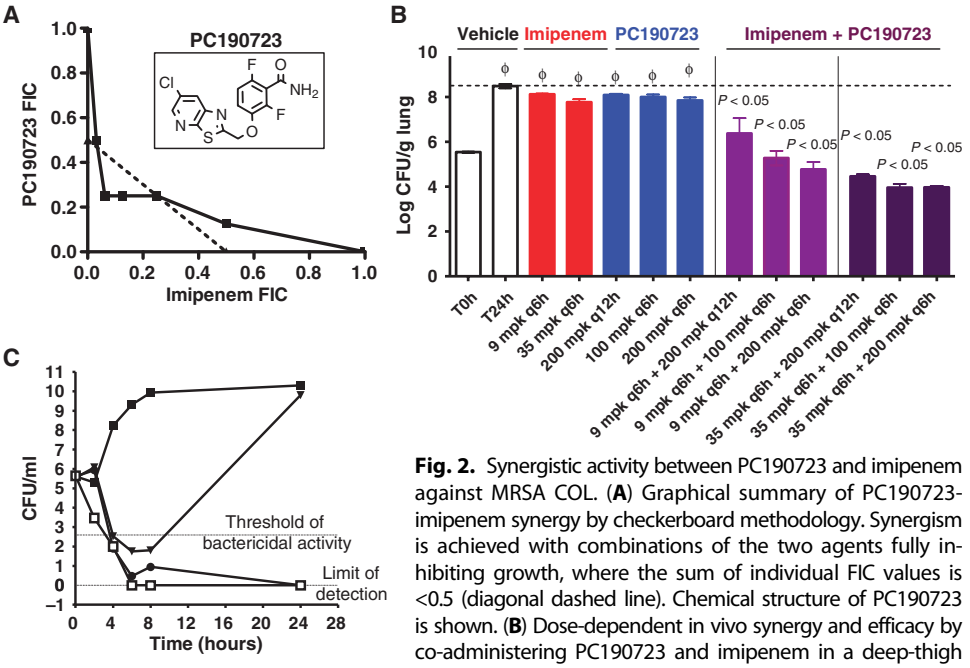

Fig. 2. Synergistic activity between PC190723 and imipenem against MRSA COL. (**A**) Graphical summary of PC190723-imipenem synergy by checkerboard methodology. Synergism is achieved with combinations of the two agents fully inhibiting growth, where the sum of individual FIC values is <0.5 (diagonal dashed line). Chemical structure of PC190723 is shown. (**B**) Dose-dependent in vivo synergy and efficacy by co-administering PC190723 and imipenem in a deep-thigh mouse model of MRSA infection. Imipenem [9 or 35 mg/kg, coformulated with cilastatin (50 mg/kg)] was infused in MRSA-infected mice for 1 hour every 6 hours (q6h), alone, or in combination with orally administered PC190723 (100 or 200 mg/kg q6h or q12h) over the 24 hours of the study. Homogenates of mouse thigh muscle were serially plated after 24-hour therapy to determine CFUs remaining in the thigh. Hashed line indicates log CFUs per thigh recovered from vehicle-treated or MRSA thigh–infected mice after 24 hours. $^{\phi}P < 0.05$ versus vehicle-treated mice at time zero (T0); $P < 0.05$, versus vehicle-treated mice at 24 hours (T24). (**C**) Time-kill curve of PC190723 against MRSA COL strain untreated (filled squares) or treated with 8× MIC of PC190723 (filled triangles and circles; two independent experiments) or the bactericidal control antibiotic levofloxacin (2× MIC empty squares).

the standard-of-care antibiotics linezolid and vancomycin (MIC_{90} for both antibiotics is 2 μg/ml). PC190723 also includes potent activity (a MIC of 0.25 μg/ml) against all linezolid-resistant, vancomycin intermediate–resistant (VISA), and vancomycin-resistant (VRSA) *S. aureus* isolates tested.

PC190723-imipenem synergy in a mouse model of MRSA

On the basis of the favorable drug-like qualities of PC190723, we tested whether its observed in vitro synergy with imipenem provided in vivo efficacy when co-administered in a murine thigh model of MRSA infection (*29*). This preclinical model of infection has been used extensively to characterize the pharmacokinetic and pharmacodynamic efficacy of antibiotics as well as to reliably predict clinical antibiotic efficacy [(*29*), and see Materials and Methods]. Individual pharmacokinetic analyses of selected doses of PC190723 and imipenem after in vivo administration in mice revealed exposures with suitable bioavailability (fig. S1). At the doses used, neither imipenem (at 9 or 35 mg/kg administered four times daily by intravenous infusion) nor PC190723 (when administered orally alone at 100 or 200 mg/kg) displayed significant efficacy as single agents in treating an MRSA infection in mice (Fig. 2B). However, co-administering these agents provided significant dose-dependent reductions in colony-forming units (CFUs) of MRSA COL versus control mock treatment at 24 hours (Fig. 2B). These depletions in CFU burden ranged from a 3.3- to 4.5-log CFU reduction when co-administering imipenem and PC190723 (Fig. 2B). As expected, control studies in this infection model confirmed in vivo synergy between imipenem and vancomycin (fig. S2A; $P < 0.05$ versus vehicle-treated mice at 24 hours) and a lack of in vivo synergy between imipenem and linezolid (fig. S2B).

Bactericidal activity of PC190723

PC190723 has been reported to have a bactericidal mode of action (*27*), meaning that drug-treated cells rapidly lose viability rather than show arrested growth (that is, a bacteriostatic effect). We confirmed these findings with PC190723-treated cells exceeding three logarithms of reduced *S. aureus* viability within 4 to 5 hours of drug treatment (Fig. 2C). Surprisingly, however, extending survival time–kill curves to 24 hours often resulted in substantial grow-back after the initial bactericidal effect. This presumably reflects the shorter (8 hours) time-kill experiments previously reported to assess PC190723 bactericidal activity (*27*) that would have missed the emergence of drug resistance mutations in this assay. Susceptibility testing of viable cells after regrowth in the 24-hour kill curve assay demonstrated a PC190723 MIC that was typically shifted >64-fold.

Molecular basis of synergy between PC190723 and β-lactam antibiotics

On the basis of the central role of FtsZ in cell division, the hypersensitivity of the *ftsZ* antisense (*ftsZ*-AS) depletion strain to β-lactam antibiotics, and the prominent synergy between PC190723 and β-lactam antibiotics, we tested whether PC190723 affects the normal localization of FtsZ and PBP2. To study localization of FtsZ, we used a previously described fluorescent derivative of FtsZ [FtsZ–cyan fluorescent protein (FtsZ-CFP)] (*30*). When expressed in MRSA COL, FtsZ-CFP correctly localized to the mid-cell and division septum (Fig. 3A and fig. S3) (*30*, *31*). However, FtsZ-CFP localization in MRSA COL was markedly altered in cells treated with PC190723 [at 10 times MIC; PC190723 (10 μg/ml)] for 30 min. FtsZ-CFP was mislocalized appearing as multiple rings and arcs without being specifically restricted to the septum (Fig. 3A and fig. S3C). MRSA COL bacteria treated with PC190723 also exhibited extensive enlargement as previously reported (*27*), indicative of FtsZ-mediated disruption of localized cell wall synthesis at the septum (*26*). Consistent with a direct effect of PC190723 on FtsZ localization, similar delocalization of FtsZ-CFP was also observed in cells treated for 30 min with PC190723 at its MIC value of 1 μg/ml (fig. S3B). In a control experiment, bacteria treated with nalidixic acid (an antibiotic targeting DNA gyrase) under the same growth inhibitory conditions did not affect FtsZ-CFP localization (fig. S5A).

We also tested localization of PBP2 in PC190723-treated MRSA COL using a newly constructed functional superfolder green fluorescent protein (sGFP)–PBP2 fusion gene integrated at the native PBP2 locus and regulated by its native promoter (see Materials and Methods). sGFP-PBP2 correctly localized to the division septum in mock-treated cells in the same way as that observed for endogenous PBP2 protein (*26*) or

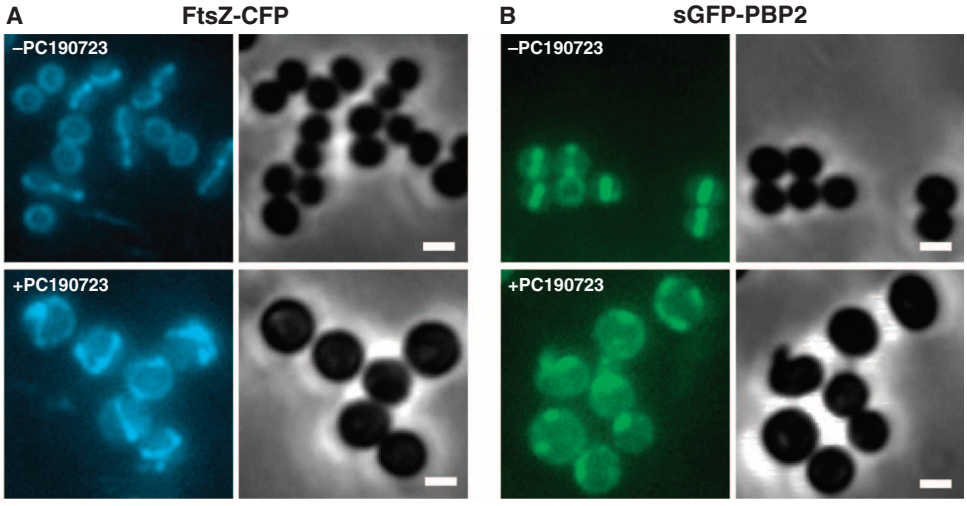

Fig. 3. Localization of FtsZ and PBP2. Septal localization of fluorescent derivatives of FtsZ and PBP2 is lost in PC190723-treated MRSA cells. (**A**) MRSA COL cells expressing FtsZ-CFP were grown in the absence (top panels) or presence of PC190723 (10 μg/ml) (bottom panels) for 30 min and analyzed by fluorescence microscopy. FtsZ-CFP fluorescence localizes to the division site in control cells versus multiple rings and arcs of FtsZ-CFP fluorescence in drug-treated cells. Right panels are companion phase-contrast images. (**B**) MRSA COL cells expressing sGFP-PBP2 were grown in the absence (top panels) or presence (bottom panels) of PC190723 as described in (A) and similarly processed for fluorescence microscopy. sGFP-PBP2 fluorescence localizes at the division site in control cells versus broad patches of sGFP-PBP2 fluorescence around the cell periphery in drug-treated cells. Right panels are companion phase-contrast images. Scale bars, 1 μm.

for a previous GFP-PBP2 construct (*31*) (Fig. 3B and fig. S4A). However, sGFP-PBP2 was extensively delocalized among cells treated with PC190723 at 1× or 10× MIC for 30 min (Fig. 3B and fig. S4BC), with discrete patches of sGFP-PBP2 localized throughout the plasma membrane. Like FtsZ-CFP, sGFP-PBP2 was correctly localized to the division site in MRSA COL cells treated with nalidixic acid (fig. S5B). Collectively, these data demonstrate that FtsZ and PBP2 are specifically delocalized from the division site of MRSA cells treated with PC190723.

Because the proper function of FtsZ and PBP2 requires precise septum localization to coordinate cell division and peptidoglycan biosynthesis, their extensive delocalization in PC190723-treated cells provides important insight into the molecular basis for the hypersensitivity of the *ftsZ*-AS MRSA strain to β-lactams as well as the chemical synergy between compounds targeting these two proteins. *ftsZ*-AS hypersensitivity to β-lactams is likely mediated by FtsZ depletion, resulting in delocalized PBP2 [as demonstrated by repression of FtsZ expression using an *S. aureus* P_{spac}-*ftsZ* conditional mutant; (*26*)], thereby substantially reducing the effective amount of β-lactam required to inhibit the residual functional activity of septum-localized PBP2. Mechanistically, PC190723 and β-lactam antibiotics are likely to be synergistic against MRSA because of the combined effects of (i) GTPase inhibition (*27*, *28*) and FtsZ delocalization, and (ii) concomitant PBP2 delocalization such that only a small amount of β-lactam antibiotic presumably is required to inactivate the residual and functional PBP2 enzyme localized at the septum.

Analysis of PC190723^R drug-resistant mutants

To further evaluate the molecular basis of PC190723 resistance, we performed an extensive drug resistance mapping analysis on the basis of 110 independent PC190723-resistant (PC190723^R) isolates across methicillin-susceptible *S. aureus* (MSSA) and various MRSA (COL, USA300, MRSA252, and Mu50) strain backgrounds. DNA sequencing revealed that all PC190723^R isolates had mutations causing amino acid substitutions that mapped to FtsZ. These included previously identified mutations (G193D, G196A, and N263K) (*27*) as well as several new mutations: F40L, E90K, Q94L, N170K, G196C, G196S, G196V, L200I, L200F, N208D, G233V, E234K, N263I, N263Y, G266D, G266V, T309I, A312E, D316E, and T329A (fig. S6). Nearly 50% of all independently derived PC190723^R mutations among MSSA strains mapped to either Gly^{193} or Gly^{196}; amino acid substitutions at either residue accounted for about 90% of PC190723-resistant MRSA isolates.

Crystal structure (2.0 Å) of *S. aureus* FtsZ-GDP in complex with PC190723

To extend the PC190723 resistance analysis, we obtained a 2.0 Å crystal structure of *S. aureus* FtsZ-GDP (guanosine diphosphate) in complex with PC190723 (Fig. 4A). Unlike the binding site predicted previously by molecular modeling studies using the *Bacillus subtilis* FtsZ protein (*27*), PC190723 binds to a narrow pocket within a deep cleft formed by the C-terminal half of the H7 helix, the T7 loop, and the C-terminal four-stranded β sheet of *S. aureus* FtsZ (Fig. 4). PC190723 inserts into this cleft in a "slab shape" with its difluorobenzamide and thiazopyridine rings almost within the same plane (Fig. 4B). PC190723 is enclosed in a mostly hydrophobic environment formed by residues from the C-terminal β sheet, T7 loop, and H7 helix. Less hydrophobic amino acids from the C-terminal β sheet are also involved in the binding (Fig. 4C). The difluorobenzamide substituent (warhead) of PC190723 fits into the top portion of the cleft by directly interacting with the T7 loop (Fig. 4B). An entity (either a water molecule or a metal ion) sits in the center of an octahedral coordination system involving five other oxygen donors: the backbone carbonyls of Leu^{200}, Leu^{209}, and Val^{203}; the side-chain carbonyl of Asn^{208}; and another water molecule at the opposite side of the difluorobenzamide carbonyl. The chlorine at the lipophilic end of PC190723 inserts into a hydrophobic tunnel formed by two residues from the H7 helix (Q192 and Gly^{193}) and two residues from the C-terminal β sheet (Met^{226} and Ile^{228}), which leads to a wide open pocket that could be structurally mapped to the equivalent of tubulin's taxol-binding site (*32*). Most key PC190723^R FtsZ mutations (for example, G193D, G196S, G196A, G196C, N263K, and L200F) map to this site, and even the most conservative change (G196A) completely occludes its entry to this site (Fig. 4, B and C). On the basis of the size constraints of the PC190723-binding pocket and the fact that it is ostensibly filled by the ligand, we conclude that the high frequency of resistance (FOR) of the compound is unlikely to be addressed through chemical modification.

PC190723 FOR

Spontaneous PC190723^R *S. aureus* mutants were isolated from agar containing PC190723 at 8× MIC or higher at a frequency of 3×10^{-8}, in

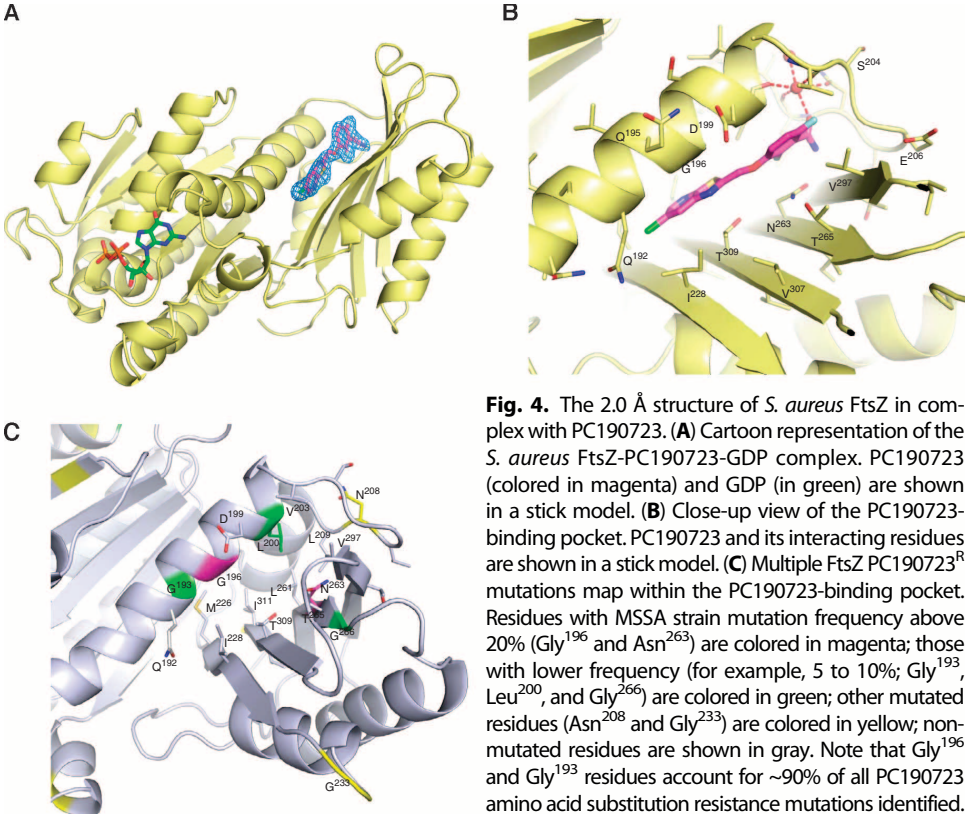

Fig. 4. The 2.0 Å structure of *S. aureus* FtsZ in complex with PC190723. (**A**) Cartoon representation of the *S. aureus* FtsZ-PC190723-GDP complex. PC190723 (colored in magenta) and GDP (in green) are shown in a stick model. (**B**) Close-up view of the PC190723-binding pocket. PC190723 and its interacting residues are shown in a stick model. (**C**) Multiple FtsZ PC190723^R mutations map within the PC190723-binding pocket. Residues with MSSA strain mutation frequency above 20% (Gly^{196} and Asn^{263}) are colored in magenta; those with lower frequency (for example, 5 to 10%; Gly^{193}, Leu^{200}, and Gly^{266}) are colored in green; other mutated residues (Asn^{208} and Gly^{233}) are colored in yellow; non-mutated residues are shown in gray. Note that Gly^{196} and Gly^{193} residues account for ~90% of all PC190723 amino acid substitution resistance mutations identified.

close agreement with previous findings (*27*). Because this FOR is borderline for development of PC190723 as a single-agent antibiotic, the FOR was also determined in the presence of the clinical breakpoint MIC (4 μg/ml) of imipenem. Under such conditions, only a 1× MIC of PC190723 was required to achieve a similar FOR (1.3×10^{-8}) as observed with PC190723 alone. A 2-fold increase in the PC190723 drug concentration in the presence of imipenem further reduced PC190723 FOR about 10-fold (1.6×10^{-9}). Therefore, pairing PC190723 with the clinical breakpoint concentration of imipenem provided a dual benefit: substantially reducing the FOR of PC190723 and restoring the efficacy of imipenem against MRSA.

Restored β-lactam susceptibility among PC190723^R FtsZ mutants

Because antisense interference of FtsZ enhances MRSA susceptibility to β-lactam antibiotics, we tested whether PC190723^R *ftsZ* mutants shared similar phenotypes. First, seven independent PC190723^R *ftsZ* mutant MRSA252 and Mu50 isolates from time-kill experiments were evaluated (table S3). Indeed, FtsZ-G196S mutants from both MRSA strain backgrounds displayed markedly reduced imipenem susceptibilities (MIC ≤0.25 μg/ml) compared to wild type (MIC ≥32 μg/ml). FtsZ-G196S mutants also displayed 4- to 128-fold greater susceptibility to penicillin (depending on strain background) but no altered susceptibility to other antibiotic classes tested (table S3). Notably, FtsZ-G196A provides an equivalent antibiotic susceptibility profile as FtsZ-G196S, unlike FtsZ-G196C, which accounts for <10% of PC190723^R isolates identified in MRSA. To access the frequency of this imipenem susceptibility phenotype among PC190723^R FtsZ mutants, we isolated nine additional independently identified mutants from MRSA COL. In total, five mutants (all FtsZ-G193D) displayed pronounced β-lactam susceptibility as determined by liquid MIC determination and agar susceptibility assay (Fig. 5, A and B). The remainder of the mutants (for example, FtsZ-G196S and FtsZ-N263Y) displayed moderate imipenem susceptibility phenotypes detected by the agar susceptibility assay. Further, penicillin susceptibility changes among PC190723^R mutants correlated with imipenem susceptibility alterations; no altered susceptibility to vancomycin was observed. Therefore, PC190723^R *ftsZ* mutants provide a continuum of enhanced β-lactam susceptibilities, but genetic modifiers likely modulate the severity of these phenotypes among different MRSA strains.

Attenuated virulence among PC190723^R imipenem^S FtsZ mutants

On the basis of the propensity of PC190723^R *ftsZ* mutants to enhance MRSA susceptibility to β-lactam antibiotics and the importance of FtsZ in cell wall biogenesis (*19*, *24*, *26*), we tested whether such mutants had growth (or fitness) phenotypes. No in vitro fitness cost was observed among multiple PC190723^R *ftsZ* mutants isolated from MRSA252 and Mu50 strain backgrounds by performing standard growth curves or competitive growth assays versus their parental wild-type control (tables S4 and S5). Because MRSA infection in the murine thigh model is benchmarked for the MRSA COL strain, we also examined whether representative PC190723^R *ftsZ* mutants in this background displayed an in vivo fitness cost (that is, virulence phenotype). Independently derived imipenem-susceptible PC190723^R *ftsZ*-G193D mutants (COL strain M2 and M4) displayed markedly reduced virulence across a range of inoculation doses, whereas two PC190723^R *ftsZ* mutants displaying more moderate imipenem susceptibility phenotypes [strain M1 (N263Y) and strain M8 (G196S)] colonized mice in a manner indistinguishable from that of the parental COL strain (Fig. 5C). Therefore, only PC190723^R mutants with a pronounced imipenem susceptibility (imipenem^S) phenotype have a concomitant attenuated virulence phenotype in a host setting, perhaps reflecting a threshold level of cell wall alterations resulting from such mutations that are necessary to effectively compromise growth and pathogenicity during infection.

Imipenem efficacy against PC190723^R imipenem^S *ftsZ* mutants

Because PC190723^R *ftsZ* mutants enhance MRSA susceptibility to β-lactam antibiotics in vitro, we also tested whether this phenotype extends to a murine infection model. Consistent with the in vitro imipenem^S phenotype of PC190723^R *ftsZ*-G193D strains M2 and M4, imipenem was also highly efficacious against these strains when dosed at 10 mg/kg subcutaneously three times daily for 24 hours, yielding a three- to four-log reduction in CFU bacterial burden versus

A

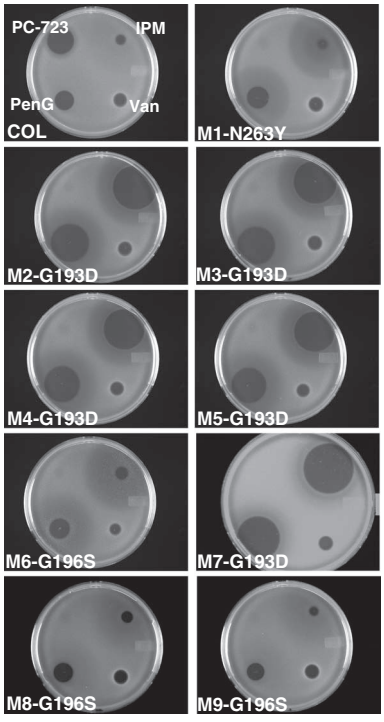

B

Strain	PC-723	IPM	Nucleotide change	Amino acid change	IPM susceptibility
COL	1	>32	NA	NA	Resistant
M1	>64	32	A788T	Asn263Tyr	Intermediate
M2	>64	<0.5	G578A	Gly193Asp	Sensitive
M3	>64	<0.5	G578A	Gly193Asp	Sensitive
M4	>64	<0.5	G578A	Gly193Asp	Sensitive
M5	>64	<0.5	G578A	Gly193Asp	Sensitive
M6	>64	>32	G586A	Gly196Ser	Intermediate
M7	>64	<0.5	G578A	Gly193Asp	Sensitive
M8	>64	>32	G586A	Gly196Ser	Resistant
M9	>64	>32	G586A	Gly196Ser	Resistant

C

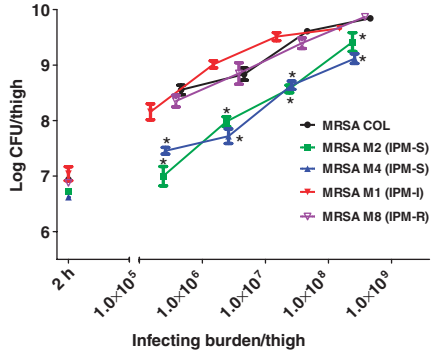

Fig. 5. Altered β-lactam susceptibility and attenuated virulence of MRSA COL PC190723^R *ftsZ* mutants. (**A**) Susceptibility of nine independently derived PC190723^R *ftsZ* mutants (M1 to M9) to PC190723 (PC-723), penicillin G (PenG), vancomycin (Van), and imipenem (IPM) using the agar susceptibility assay. (**B**) Summary of nucleotide changes and amino acid substitutions of PC190723^R *ftsZ* mutants M1 to M9 described in (A). PC190723 and imipenem susceptibility of M1 to M9 mutants are summarized as MIC values and qualitative imipenem susceptibility phenotype. (**C**) Attenuated virulence of PC190723^R imipenem^S *ftsZ*-G193D mutants M2 and M4 across escalating infection doses. PC190723^R mutants M1 and M8 display intermediate (IPM-I) or strong resistance (IPM-R) to imipenem, respectively, and are fully virulent versus the parental MRSA COL strain. *$P < 0.05$ versus MRSA COL.

mock-treated control groups administered vehicle (10 mM MOPS) or the imipenem-resistant parental COL strain identically treated with imipenem (Fig. 6). Conversely, imipenem administered under these same conditions lacked any detectable efficacy against PC190723^R *ftsZ* mutants (M1, N263Y and M8, G196S) that display only minor in vitro changes in imipenem susceptibility (Fig. 6). Considering that >75% of all MRSA PC190723^R mutations correspond to G193D, G196S, or G196A (fig. S6) and such mutations share a propensity to most markedly enhance imipenem susceptibility despite strain-to-strain variation (*33*, *34*) (Fig. 5 and table S3), PC190723 FOR is reduced concomitant with therapeutic conditions in which imipenem is co-administered.

DISCUSSION

MRSA remains one of the leading causes of nosocomial infection worldwide, and alternative therapeutic strategies are urgently needed (*2*, *7*, *35*, *36*). Here, we describe a general strategy to identify new agents that, when paired with existing β-lactams, restore the efficacy of this important antibiotic class against MRSA. Our approach first relies on antisense interference to identify targets whose partial depletion is sufficient to substantially restore MRSA susceptibility to β-lactams (*16*). Cognate inhibitors to such targets are predicted to display synergistic activity in combination with β-lactams. Target-based resistance to such new agents is also predicted to potentially recapitulate the β-lactam hypersusceptibility phenotype originally demonstrated by antisense interference, thereby making such targets desirable from the perspective of mitigating drug resistance and the rational design of new antibiotic combination agents.

We demonstrate these principles through genetic and chemical modulation of the *S. aureus* cell division protein FtsZ. Consistent with the restored MRSA susceptibility to β-lactams demonstrated by antisense depletion of FtsZ (and other cell division proteins including FtsA and FtsW), the potent and selective FtsZ inhibitor PC190723 (*27*) displays strong synergy specifically in combination with β-lactam antibiotics. Further, co-administering imipenem and PC190723 results in strong in vivo synergy and efficacy in a murine model of MRSA infection (in which the MRSA strain is injected into the thigh muscle) under conditions where neither agent alone is efficacious using identical dosing regimens. PC190723^R mutants map exclusively to the *ftsZ* gene. A 2 Å co-crystal structure of the *S. aureus* FtsZ protein in complex with PC190723 demonstrates that FtsZ amino acid substitutions in PC190723^R mutants map largely to the ligand-binding site and are predicted to prevent PC190723 from binding to the protein. Notwithstanding the difficulty of chemical optimization of PC190723 to overcome this issue, several FtsZ amino acid substitution mutations in multiple MRSA strain backgrounds display restored β-lactam susceptibility as well as an attenuated virulence phenotype, thus effectively reducing the frequency of PC190723^R mutants and enhancing the efficacy of imipenem when the two agents are used in combination.

These findings have broad significance for antibacterial drug discovery. Beyond FtsZ, our genetic approach identifies a diverse set of additional β-lactam potentiation targets (*16*) for which cognate inhibitors are similarly predicted to be synergistic when paired with existing β-lactams. PC190723^R mutants often confer a restored β-lactam susceptibility phenotype mirroring the original phenotype obtained after genetically depleting *ftsZ* in MRSA. Therefore, drug-resistant mutants to cognate inhibitors of other β-lactam susceptibility determinants may similarly share this phenotype, which is beneficial in the context of a β-lactam potentiation agent. We also demonstrate that the FOR of PC190723 is substantially (10-fold) reduced when this drug is combined with a β-lactam antibiotic because of the restored

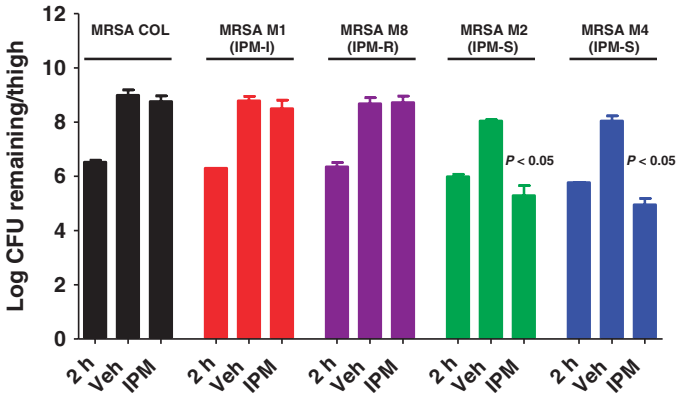

Fig. 6. Restored efficacy of imipenem against PC190723^R imipenem^S *ftsZ*-G193D mutants in a mouse deep-thigh infection model of MRSA. Efficacy studies were performed as described in Fig. 2B using PC190723^R imipenem^S *ftsZ*-G193D mutants M2 and M4 versus PC190723^R *ftsZ*-N263Y mutant M1 (IPM-I), PC190723^R *ftsZ*-G196S mutant M8 (IPM-R), and the parental MRSA COL strain. Bacterial burden was enumerated and compared among three groups: imipenem (IPM) treatment, 2 hours after infection, and the vehicle (Veh) control group. $P < 0.05$, versus respective thigh bacterial burden in 24-hour control vehicle.

β-lactam susceptibility of many of the PC190723^R mutants. Therefore, antibiotic leads targeting other β-lactam susceptibility determinants and that lack a satisfactory resistance profile required for their progression as a single agent may similarly be paired with a β-lactam to address drug resistance issues. "Repurposing" antibiotic leads such as PC190723 in this manner provides an important opportunity for a combination-agent strategy applied to Gram-positive drug-resistant bacteria. The combination-agent strategy would involve target-inhibitor classes distinct from the β-lactamase–β-lactamase inhibitors that have proven clinically successful against Gram-negative drug-resistant bacteria (*6*).

A fundamental question arising from our work is the molecular basis of synergy between PC190723 and β-lactams, a phenomenon observed both in vitro (across 51 MRSA clinical isolates tested) (table S2) and in a murine model of MRSA. Indeed, this question is particularly challenging to address because the central role of FtsZ involves, directly or indirectly, the spatial and temporal recruitment of most (if not all) of the proteins that make up the divisome, therefore affecting cell wall biogenesis processes including completion of peptidoglycan biosynthesis, cross-linking, and presumably cell wall degradation during cell septation (*19*, *20*, *23*, *25*, *26*, *31*). Notwithstanding this complexity, an important clue to the basis of the observed synergy between these agents is that FtsZ is required for PBP2 localization in *S. aureus* (*31*) as well as proper localization of PBPs in other bacteria (*37*, *38*). These data, combined with the marked hypersensitivity of the *ftsZ*-AS depletion strain to β-lactams, prompted us to examine the localization of these proteins in PC190723-treated cells. It has been demonstrated that in *B. subtilis* cells, PC190723 treatment results in delocalization of FtsZ from the division septum, with the protein appearing as discrete foci present throughout the cell (*27*). We show that FtsZ is also highly delocalized in PC190723-treated MRSA COL, forming multiple rings or arcs. Markedly, however, PBP2 is also delocalized in PC190723-treated MRSA cells. Because MRSA β-lactam resistance is mediated through the cooperative function of PBP2 and PBP2A to carry out peptidoglycan biosynthesis and cross-linking (*10*), PBP2 delocalization in PC190723-treated cells would be expected to confer crippling effects particularly against MRSA in the presence of a β-lactam antibiotic.

We postulate that the synergy observed between these agents is (at least in part) the result of PC190723-mediated inhibition and delocalization of FtsZ, which in turn causes PBP2 delocalization so that a substantially reduced effective concentration of the β-lactam is required to inhibit the residual functional and correctly localized PBP2. Synergy between PC190723 and β-lactams may also be amplified by additional factors. For example, FtsZ is also required for correct septum localization of FtsW (*39*), which translocates peptidoglycan precursor substrate from the cytoplasm to the extracellular cell wall (*40*). Because PBP2 recruitment to the division site is also mediated by its association with peptidoglycan precursors (*31*), FtsZ-mediated delocalization of FtsW could similarly enhance the activity of β-lactams in the presence of PC190723. Indeed, β-lactams themselves, which acylate the transpeptidation active site of PBPs, are reported to delocalize *S. aureus* PBP2 (*31*) and may also affect the localization of other PBPs. Moreover, multiple cell wall biogenesis genes directly involved in peptidoglycan and teichoic acid synthesis (i) are as hypersensitive to β-lactams as mutants derived by antisense-based depletion or gene deletion (*15*–*18*, *41*, *42*) and (ii) express proteins that also localize to the division site in an FtsZ-dependent manner (*25*, *26*, *31*). The molecular basis of chemical synergy between PC190723 and β-lactams is highly complex, but it is precisely the complexity of this interdependent network of functional interactions between FtsZ, downstream divisome components, and cell wall biosynthetic enzymes that provides an "Achilles' heel" to exploit and potentially develop alternative combination-agent strategies against MRSA.

In summary, a chemical-genetic approach to identifying new targets that buffer MRSA bacteria from existing antibiotics has important implications in developing effective antibiotic combination agents. Chemical-genetic interaction networks predict compound synergy between cognate inhibitors of such targets and their corresponding companion antibiotic (*15*, *16*). Analogous to any genetic strategy to identify targets that display restored antibiotic susceptibility phenotypes, we demonstrate that spontaneous drug-resistant mutations to cognate inhibitors of such targets can also recapitulate this antibiotic susceptibility phenotype and reduce the impact of antibiotic resistance in the context of combination agents. Further, mutations that confer resistance to the potentiating agent may compromise the virulence of the pathogen, again reducing the impact of drug resistance with combination therapeutics. Like FtsZ and PC190723, inhibitors to other essential gene products that make up the MRSA chemical genetic interaction network of imipenem are also predicted to serve as β-lactam potentiating agents with similar therapeutic advantages.

MATERIALS AND METHODS

Microbiological studies

All studies use MRSA COL (MB5393), MRSA 252 (MB6259), or MRSA Mu50 (MB6258). MRSA COL is a hospital-acquired penicillinase-negative strain extensively used in biochemical and genetic investigations of *S. aureus* methicillin resistance (*16*, *17*) and from which its genome has been fully sequenced and annotated (*43*). MICs were determined by the broth microdilution method according to the recommendations of the Clinical and Laboratory Standards Institute (*44*).

The standard checkerboard technique was used to quantify synergy between antibiotic agents (*45*). MB5393 was grown in cation-adjusted Mueller-Hinton broth (CAMHB) medium and assayed in a 96-well format with twofold dilutions of PC190723 and drugs listed in table S1. MIC determinations were assessed visually. Fractional inhibitory concentration index (FICI) values were determined by adding the FIC value of each compound required to achieve a MIC when paired with the second agent.

Time-kill studies

Bacterial survival assays were performed with MRSA COL cells grown to mid-logarithmic phase and diluted to about 5×10^5 CFUs/ml in CAMHB containing various concentrations of PC190723. Cultures were incubated at 37°C with shaking. At the indicated time points, 100 µl of samples was removed for serial dilution in 900 µl of sterile saline solution and 100 µl of aliquots from the three dilutions spread on to brain heart infusion agar (BHIA) plates. Cell counts (CFUs/ml) were enumerated after incubating plates at 37°C for 18 hours.

Isolation of PC190723^R mutants

Cells of MRSA COL (MB5393), MRSA 252 (MB6259), or MRSA Mu50 (MB6258) were grown to late-exponential phase [optical density at 600 nm (OD_{600}) ~1.0; ~10^9 CFUs/ml] and spread on BHIA plates containing twofold escalating agar MIC levels of PC190723. To establish the number of viable cells in the starting inoculum, we serially diluted and plated the culture to BHIA plates lacking PC190723. Resistant isolates were restreaked on plates containing the same PC190723 concentration. The FOR was determined by dividing the number of resistant isolates by the viable CFUs in the late-exponential inoculum.

Competitive growth assays

Parental wild-type and corresponding mutant strains were grown overnight in LB medium at 37°C. Cultures were diluted to ~5×10^5 CFUs/ml in 2 ml of fresh LB medium. Individual mutant and parental wild-type strains were mixed at a 1:1 ratio with final volume of 2 ml and grown for 48 hours at 37°C with shaking. At the 24-hour time point, 40 µl of each coculture was transferred to 2 ml of fresh LB (50× dilution) and incubated for another 24 hours. Ratios between strains were determined by enumerating CFUs after serial dilution on LB agar plates with or without PC190723 (4 µg/ml). If the CFU difference between PC190723 plus and minus is less than fivefold over 48-hour growth, we conclude that the mutant lacks a clear fitness or growth defect relative to wild-type growth.

Antisense interference studies

A detailed description of all antisense interference fragments, including DNA sequence, BLAST scores of best *S. aureus* match, and gene nomenclature in MSSA strain RN4220 and MRSA COL, has been previously reported (*16*). MRSA COL was transformed with antisense interference plasmids or vector control as previously described (*15*). Assay plates were prepared by seeding 10^7 cells/ml of each culture into 48°C cooled LB-Miller agar containing chloramphenicol (34 µg/ml) and 0, 25, 50, 100, or 200 mM xylose. Agar plates were allowed to set and then spotted with 10 µl of each drug and incubated at 37°C with humidity for 18 hours.

Agar susceptibility assay

Parental wild-type and corresponding mutant strains were inoculated in LB medium overnight at 37°C. Culture was then diluted to about 5×10^6 CFUs/ml with 20 ml of 46°C LB agar (1.2% agar concentration) and poured/plated immediately and allowed to cool. Five microliters of compound was then spotted. Final amounts of PC190723, penicillin G, imipenem, and vancomycin were 2.8, 16.0, 8.0, and 2.0 µg, respectively. Plates were incubated for 16 hours at 37°C, and photos were subsequently taken.

Animal efficacy studies

A late-exponential phase (OD_{600} ~1.0; ~10^9 CFUs/ml) overnight culture of MRSA COL (MB 5393) in trypticase soy broth (TSB) medium was serially diluted for intramuscular thigh inoculation (~10^7 CFUs/ml; 0.1 ml per injection). Two hours after infection, MRSA thigh–infected jugular-cannulated female CD-1 mice were administered vehicle, monotherapy, or combination therapy. Thigh homogenates were serially plated 24 hours after initiation of therapy to determine CFUs per thigh remaining. To demonstrate in vivo synergy between the two agents, we first determined clinically relevant imipenem doses, which are minimally efficacious against MRSA COL. Plasma protein binding in human and female CD-1 mouse was measured by the equilibrium dialysis method, and the unbound fraction was 80 and 52%, respectively. The blood/plasma ratio of imipenem was measured to be 0.52 in female CD-1 mouse. To achieve the same unbound area under the curve (AUC) in mouse plasma as in human plasma, a dose (35 mg/kg) in mouse (infused intravenously) would represent a human dose of 250 mg (table S6). Doses of 64 and 123 mg/kg (infused intravenously) would represent human doses of 500 and 1000 mg, respectively (table S6). In mice, imipenem [9 or 35 mg/kg per infusion (representative of a 250-mg human dose)], coformulated with cilastatin (50 mg/kg) (the inhibitor of the renal dipeptidase, dehydropeptidase I) in 10 mM MOPS buffer, was infused alone intravenously for 1 hour every 6 hours over the 24-hour study (q6h). Mouse tail blood samples (15 µl) were added to 45 µl of 0.1 M trisodium citrate buffer and then stabilized by the addition of 60 µl of a 1:1 mixture of 1 M MES buffer (pH 6.0) and 50% ethylene glycol, and stored at −80°C until liquid chromatography–mass spectrometry analysis. Pharmacokinetic analysis demonstrated that the plasma levels (free concentrations) of imipenem did not exceed its MIC when infused at 9 mg/kg q6h, whereas imipenem exceeded its MIC about 22% over 24 hours when infused at 35 mg/kg q6h (T > MIC ~22%, fig. S1). Accordingly, minimal efficacy of imipenem was observed after 24 hours in vivo versus MRSA in thigh-infected mice (Fig. 2B). Similarly, PC190723 when administered alone orally at 100 or 200 mg/kg q6h or q12h displayed marginal efficacy on its own (Fig. 2B), despite its demonstrated efficacy at lower doses in a murine septicemia model with *S. aureus* strain Smith (*27*). However, when these agents were combined at these doses, a synergistic, antibacterial efficacy compared to vehicle-treated, infected animals was observed, ranging from 2.2-log CFU reduction when co-administering imipenem at 9 mg/kg q6h and PC190723 at 200 mg/kg q12h to a 4.5-log CFU reduction with imipenem at 35 mg/kg q6h and PC190723 at 200 mg/kg q6h (Fig. 2B). Control studies to evaluate in vivo synergy between imipenem and vancomycin (fig. S2A) or imipenem combined with linezolid were similarly performed (fig. S2B). Briefly, a late-exponential phase (OD_{600} ~1.0; ~10^9 CFUs/ml) overnight culture of MRSA COL (MB 5393) in TSB medium was serially diluted for intramuscular thigh inoculation (~10^7 CFUs/ml; 0.1 ml per injection). Two hours after infection, MRSA thigh–infected mice were administered vancomycin (5 or 10 mg/kg, twice daily) or linezolid (10 or 20 mg/kg, twice daily) in the absence or presence of a nonefficacious dose of imipenem (100 mg/kg, via subcutaneously implanted osmotic minipumps). Thigh homogenates were

serially plated 24 hours after initiation of therapy to determine CFUs per thigh remaining. All animal experiments were performed according to Merck and American Association for Accreditation of Laboratory Animal Care guidelines for the ethical treatment of animals.

In vivo virulence studies of PC190723^R isolates

Cultures of MRSA COL (MB 5393) in TSB medium and PC190723^R strains [PC190723^R IPM-S (M2), PC190723^R IPM-S (M4), PC190723^R IPM-R (M1), and PC190723^R IPM-R (M8)] in TSB medium supplemented with PC190723 (10 μg/ml) were grown overnight to late-exponential phase (OD_{600} ~1.0; ~10^9 CFUs/ml). Five groups of mice were thigh-inoculated (0.1 ml per injection) with an isolate, each at increasing inoculum concentrations ranging from ~10^5 to 10^9 CFUs/ml. Thigh homogenates were serially plated 24 hours after infection to determine CFUs per thigh remaining.

Fluorescence microscopy and cellular localization studies of FtsZ-CFP and sGFP-PBP2 drug-treated MRSA

To construct an *S. aureus* COL strain where the native *pbpB* gene, encoding PBP2, was replaced by a *sfgfp-pbpB* fusion, we constructed a plasmid where we introduced the *sfgfp* gene, encoding the superfolder GFP variant (*46*), between the *recU* and the *pbpB* genes. For that purpose, we first amplified the upstream region of *pbpB* (primers BCBP5 and BCBP6) and the 5′ region of the *pbpB* gene (primers BCBP7 and BCBP8). The *sfgfp* gene was amplified from plasmid pTRC99a-P5 (*46*) (primers BCBP9 and BCBP10). A sequence encoding a 12–amino acid linker was introduced between the *sfgfp* and the *pbpB* genes (sequence underlined in primers BCBP8 and BCBP10). The three fragments were joined by overlap polymerase chain reaction (PCR) in two steps and cloned into pBCBPM016, resulting in plasmid pBCBPM061. The pBCBPM016 plasmid is a derivative from the pMAD vector (*47*), in which the erythromycin resistance cassette was replaced by a kanamycin resistance cassette obtained from the pDG792 plasmid (*48*). Plasmid pBCBPM061 was sequenced, electroporated into *S. aureus* RN4220 strain as previously described (*49*), and transduced into *S. aureus* COL strain with phage 80α (*50*). Insertion and excision of pBCBPM061 into the chromosome of *S. aureus* COL strain were performed as previously described (*47*). The replacement of the native *pbpB* gene by the *sfgfp-pbpB* gene fusion was confirmed by PCR (with primers BCBP11 and BCBP12). The resulting strain, named BCBPM073, expresses an sGFP fusion to PBP2, from its native chromosomal locus, under the control of its native promoter.

To construct an *S. aureus* COL strain ectopically expressing an FtsZ-CFP fusion from the *spa* locus of *S. aureus* chromosome, under the control of the P_{spac} promoter, we transduced the pBCBHV003 plasmid (*30*) into strain COL. Insertion and excision of pBCBHV003 into the chromosome of COL allowed the replacement of the *spa* gene by the *ftsZ-cfp* fusion, generating strain BCBAJ020.

For fluorescence microscopy studies, *S. aureus* strains BCBPM073 (expressing sGFP-PBP2) and BCBAJ020 (expressing FtsZ-CFP) were inoculated in TSB at 37°C for 18 hours. The cultures were then diluted 1:200 into fresh TSB supplemented with 0.1 mM isopropyl-β-D-thiogalactopyranoside (IPTG) when required and further incubated in the same conditions. At mid-exponential phase (OD_{600} 0.6 to 0.8), cultures were divided into prewarmed flasks and either PC190723 or nalidixic acid was added at 1× or 10× the corresponding MIC values for each compound. Flasks to which no antibiotic was added were used as controls for the experiment. Bacterial cultures were then incubated for 30 min, after which aliquots were collected, pelleted, and washed with phosphate-buffered saline (PBS). Cells were mounted on a microscope slide covered with a thin film of 1% agarose in PBS and observed by fluorescence microscopy with a Zeiss Axio observer Z1 microscope. Image acquisition was performed with a Photometrics CoolSNAP HQ2 camera (Roper Scientific) and MetaMorph 7.5 software (Molecular Devices). Primer sequences used in the strain constructions are the following: BCBP5, cgcgGGATCCcgtgtatgttgttatacgatgaaaa; BCBP6, tcatacgcggtcctcactttcatctaatatcaacttatcaac; BCBP7, cgcGGATCCcttgtagaagctaccattatcaaca; BCBP8, actagtggtggaggaggttctggtggaggaggttctatgacggaaaacaaaggatcttctcagcc; BCBP9, aaagtgaggaccgcgtatgactagtagtaaaggagaagaac; BCBP10, agaacctcctccaccagaacctcctccaccactagtgtcgactttgtatagttcatccatgccatg; BCBP11, ggtggacgtggtatgtcac; and BCBP12, tgcaataatcatgaagcc.

Restored efficacy of imipenem against PC190723^R imipenem^S *ftsZ*-G193D mutants in a deep-thigh infection model

Female CD-1 mice inoculated into the thighs with overnight cultures (~10^6 CFUs per thigh) of MRSA COL, representative PC190723^R *ftsZ* mutants displaying imipenem susceptibility (M2 and M4), or more moderate imipenem susceptibility (M1 and M8) were treated with vehicle or imipenem (10 mg/kg per dose × 3 over 24 hours). Thigh homogenates were serially plated after 2 or 24 hours (vehicle, imipenem) to determine CFUs per thigh remaining.

X-ray crystallographic structural studies of *S. aureus* FtsZ in complex with PC190723

N-terminal His-tagged *S. aureus* FtsZ [19 mg/ml in 25 mM tris (pH 7.0), 100 mM NaCl buffer] was crystallized by sitting-drop vapor-diffusion method with 0.1 M ammonium sulfate, 0.1 M tris (pH 8.5), and 25% polyethylene glycol 3350 as the precipitating agent. Crystals were soaked with 1 mM PC190723 for 1 to 3 days before freezing in liquid nitrogen for data collection at the Industrial Macromolecular Crystallography Association (IMCA) beamline (Argonne National Labs, The Advanced Photon Source) with an x-ray wavelength of 1.00 Å. Data were integrated and reduced with the XDS program (*51*) (table S7). The structure was determined by molecular replacement with the previously determined *S. aureus* FtsZ-GDP structure (which will be reported elsewhere) as a starting model for rigid-body refinement with REFMAC (*52*) as implemented in CCP4 (*53*). The model was built manually with Coot (*54*) and completed with iterative rounds of refinement and rebuilding. The final model has R/R_{free} values of 18.8 and 22.2%, and has excellent geometry and stereochemistry. The MolProbity score (*55*) is 1.68, and 98.03% of the residues lie in the most favored region of the Ramachandran plot, as calculated by MolProbity. The final structure has been deposited with the Research Collaboratory for Structural Bioinformatics (RCSB) Protein Data Bank, ID code (pending #4DXD). Structure determination statistics are provided in table S7. Figure 3 was prepared with the program PyMOL (*56*).

SUPPLEMENTARY MATERIALS

www.sciencetranslationalmedicine.org/cgi/content/full/4/126/126ra35/DC1

Fig. S1. Pharmacokinetic profiles of imipenem and PC190723 in mice.

Fig. S2. Combination therapy in mice.

Fig. S3. Large-field fluorescence image of FtsZ-CFP cellular localization in control and PC190723-treated MRSA COL.

Fig. S4. Large-field fluorescence image of sGFP-PBP2 cellular localization in control and PC190723-treated MRSA COL.

Fig. S5. Septal localization of FtsZ-CFP and sGFP-PBP2 is unaltered in nalidixic acid–treated MRSA cells.
Fig. S6. Summary of PC190723-resistant mutants that map to FtsZ.
Table S1. Summary of in vitro synergy between PC190723 and diverse antibiotic drug classes.
Table S2. Summary of PC190723 activity across a panel of 105 clinical isolates of *S. aureus*.
Table S3. Summary of imipenem susceptibility studies on PC190723-resistant mutants isolated from MRSA252 and MRSA Mu50 strain backgrounds.
Table S4. Summary of growth rates in LB medium for strains described in table S3.
Table S5. Summary of competitive growth rates for strains described in table S3.
Table S6. Pharmacokinetic calculations for determining the appropriate imipenem dose for MRSA infection model studies in female CD-1 mice.
Table S7. *S. aureus* FtsZ structure determination statistics.

REFERENCES AND NOTES

1. C. Walsh, *Antibiotics: Actions, Origins, Resistance* (ASM Press, Washington, DC, 2003).
2. H. W. Boucher, G. H. Talbot, J. S. Bradley, J. E. Edwards, D. Gilbert, L. B. Rice, M. Scheld, B. Spellberg, J. Bartlett, Bad bugs, no drugs: No ESKAPE! An update from the Infectious Diseases Society of America. *Clin. Infect. Dis.* **48**, 1–12 (2009).
3. L. I. Llarrull, S. A. Testero, J. F. Fisher, S. Mobashery, The future of the β-lactams. *Curr. Opin. Microbiol.* **13**, 551–557 (2010).
4. G. Devasahayam, W. M. Scheld, P. S. Hoffman, Newer antibacterial drugs for a new century. *Expert Opin. Investig. Drugs* **19**, 215–234 (2010).
5. H. de Lencastre, D. Oliveira, A. Tomasz, Antibiotic resistant *Staphylococcus aureus*: A paradigm of adaptive power. *Curr. Opin. Microbiol.* **10**, 428–435 (2007).
6. S. M. Drawz, R. A. Bonomo, Three decades of β-lactamase inhibitors. *Clin. Microbiol. Rev.* **23**, 160–201 (2010).
7. R. M. Klevens, M. A. Morrison, J. Nadle, S. Petit, K. Gershman, S. Ray, L. H. Harrison, R. Lynfield, G. Dumyati, J. M. Townes, A. S. Craig, E. R. Zell, G. E. Fosheim, L. K. McDougal, R. B. Carey, S. K. Fridkin; Active Bacterial Core surveillance (ABCs) MRSA Investigators, Invasive methicillin-resistant *Staphylococcus aureus* infections in the United States. *JAMA* **298**, 1763–1771 (2007).
8. B. J. Hartman, A. Tomasz, Low-affinity penicillin-binding protein associated with β-lactam resistance in *Staphylococcus aureus*. *J. Bacteriol.* **158**, 513–516 (1984).
9. M. Matsuhashi, M. D. Song, F. Ishino, M. Wachi, M. Doi, M. Inoue, K. Ubukata, N. Yamashita, M. Konno, Molecular cloning of the gene of a penicillin-binding protein supposed to cause high resistance to β-lactam antibiotics in *Staphylococcus aureus*. *J. Bacteriol.* **167**, 975–980 (1986).
10. M. G. Pinho, H. de Lencastre, A. Tomasz, An acquired and a native penicillin-binding protein cooperate in building the cell wall of drug-resistant staphylococci. *Proc. Natl. Acad. Sci. U.S.A.* **98**, 10886–10891 (2001).
11. M. G. Pinho, S. R. Filipe, H. de Lencastre, A. Tomasz, Complementation of the essential peptidoglycan transpeptidase function of penicillin-binding protein 2 (PBP2) by the drug resistance protein PBP2A in *Staphylococcus aureus*. *J. Bacteriol.* **183**, 6525–6531 (2001).
12. D. Lim, N. C. Strynadka, Structural basis for the β lactam resistance of PBP2a from methicillin-resistant *Staphylococcus aureus*. *Nat. Struct. Biol.* **9**, 870–876 (2002).
13. L. L. Silver, Challenges of antibacterial discovery. *Clin. Microbiol. Rev.* **24**, 71–109 (2011).
14. R. A. Forsyth, R. J. Haselbeck, K. L. Ohlsen, R. T. Yamamoto, H. Xu, J. D. Trawick, D. Wall, L. Wang, V. Brown-Driver, J. M. Froelich, G. C. Kedar, P. King, M. McCarthy, C. Malone, B. Misiner, D. Robbins, Z. Tan, Z. Zhu, G. Carr, D. A. Mosca, C. Zamudio, J. G. Foulkes, J. W. Zyskind, A genome-wide strategy for the identification of essential genes in *Staphylococcus aureus*. *Mol. Microbiol.* **43**, 1387–1400 (2002).
15. J. Huber, R. G. Donald, S. H. Lee, L. W. Jarantow, M. J. Salvatore, X. Meng, R. Painter, R. H. Onishi, J. Occi, K. Dorso, K. Young, Y. W. Park, S. Skwish, M. J. Szymonifka, T. S. Waddell, L. Miesel, J. W. Phillips, T. Roemer, Chemical genetic identification of peptidoglycan inhibitors potentiating carbapenem activity against methicillin-resistant *Staphylococcus aureus*. *Chem. Biol.* **16**, 837–848 (2009).
16. S. H. Lee, L. W. Jarantow, H. Wang, S. Sillaots, H. Cheng, T. C. Meredith, J. Thompson, T. Roemer, Antagonism of chemical genetic interaction networks resensitize MRSA to β-lactam antibiotics. *Chem. Biol.* **18**, 1379–1389 (2011).
17. H. De Lencastre, S. W. Wu, M. G. Pinho, A. M. Ludovice, S. Filipe, S. Gardete, R. Sobral, S. Gill, M. Chung, A. Tomasz, Antibiotic resistance as a stress response: Complete sequencing of a large number of chromosomal loci in *Staphylococcus aureus* strain COL that impact on the expression of resistance to methicillin. *Microb. Drug Resist.* **5**, 163–175 (1999).
18. B. Berger-Bächi, S. Rohrer, Factors influencing methicillin resistance in staphylococci. *Arch. Microbiol.* **178**, 165–171 (2002).
19. D. J. Scheffers, M. G. Pinho, Bacterial cell wall synthesis: New insights from localization studies. *Microbiol. Mol. Biol. Rev.* **69**, 585–607 (2005).
20. D. W. Adams, J. Errington, Bacterial cell division: Assembly, maintenance and disassembly of the Z ring. *Nat. Rev. Microbiol.* **7**, 642–653 (2009).
21. S. G. Addinall, E. Bi, J. Lutkenhaus, FtsZ ring formation in *fts* mutants. *J. Bacteriol.* **178**, 3877–3884 (1996).
22. H. P. Erickson, D. E. Anderson, M. Osawa, FtsZ in bacterial cytokinesis: Cytoskeleton and force generator all in one. *Microbiol. Mol. Biol. Rev.* **74**, 504–528 (2010).
23. A. Zapun, T. Vernet, M. G. Pinho, The different shapes of cocci. *FEMS Microbiol. Rev.* **32**, 345–360 (2008).
24. B. Lara, D. Mengin-Lecreulx, J. A. Ayala, J. van Heijenoort, Peptidoglycan precursor pools associated with MraY and FtsW deficiencies or antibiotic treatments. *FEMS Microbiol. Lett.* **250**, 195–200 (2005).
25. M. L. Atilano, P. M. Pereira, J. Yates, P. Reed, H. Veiga, M. G. Pinho, S. R. Filipe, Teichoic acids are temporal and spatial regulators of peptidoglycan cross-linking in *Staphylococcus aureus*. *Proc. Natl. Acad. Sci. U.S.A.* **107**, 18991–18996 (2010).
26. M. G. Pinho, J. Errington, Dispersed mode of *Staphylococcus aureus* cell wall synthesis in the absence of the division machinery. *Mol. Microbiol.* **50**, 871–881 (2003).
27. D. J. Haydon, N. R. Stokes, R. Ure, G. Galbraith, J. M. Bennett, D. R. Brown, P. J. Baker, V. V. Barynin, D. W. Rice, S. E. Sedelnikova, J. R. Heal, J. M. Sheridan, S. T. Aiwale, P. K. Chauhan, A. Srivastava, A. Taneja, I. Collins, J. Errington, L. G. Czaplewski, An inhibitor of FtsZ with potent and selective anti-staphylococcal activity. *Science* **321**, 1673–1675 (2008).
28. J. M. Andreu, C. Schaffner-Barbero, S. Huecas, D. Alonso, M. L. Lopez-Rodriguez, L. B. Ruiz-Avila, R. Núñez-Ramírez, O. Llorca, A. J. Martín-Galiano, The antibacterial cell division inhibitor PC190723 is an FtsZ polymer-stabilizing agent that induces filament assembly and condensation. *J. Biol. Chem.* **285**, 14239–14246 (2010).
29. C. J. Gill, G. K. Abruzzo, A. M. Flattery, A. S. Misura, K. Bartizal, E. J. Hickey, In vivo efficacy of a novel oxazolidinone compound in two mouse models of infection. *Antimicrob. Agents Chemother.* **51**, 3434–3436 (2007).
30. H. Veiga, A. M. Jorge, M. G. Pinho, Absence of nucleoid occlusion effector Noc impairs formation of orthogonal FtsZ rings during *Staphylococcus aureus* cell division. *Mol. Microbiol.* **80**, 1366–1380 (2011).
31. M. G. Pinho, J. Errington, Recruitment of penicillin-binding protein PBP2 to the division site of *Staphylococcus aureus* is dependent on its transpeptidation substrates. *Mol. Microbiol.* **55**, 799–807 (2005).
32. J. Löwe, H. Li, K. H. Downing, E. Nogales, Refined structure of αβ-tubulin at 3.5 Å resolution. *J. Mol. Biol.* **313**, 1045–1057 (2001).
33. Genetic modifiers of this phenotype perhaps among a partner protein to which FtsZ physically interacts may directly or indirectly contribute to the imipenem susceptibility phenotypes we observe. More subtle differences within the cell division protein network may also vary across MRSA isolates because comparative genomics studies among sequenced genomes of strains used in this study (MRSA COL, MRSA252, Mu50, and USA300) underscore extensive genetic variation between *S. aureus* isolates (*34*).
34. Y. Feng, C. J. Chen, L. H. Su, S. Hu, J. Yu, C. H. Chiu, Evolution and pathogenesis of *Staphylococcus aureus*: Lessons learned from genotyping and comparative genomics. *FEMS Microbiol. Rev.* **32**, 23–37 (2008).
35. R. Köck, K. Becker, B. Cookson, J. E. van Gemert-Pijnen, S. Harbarth, J. Kluytmans, M. Mielke, G. Peters, R. L. Skov, M. J. Struelens, E. Tacconelli, A. Navarro Torné, W. Witte, A. W. Friedrich, Methicillin-resistant *Staphylococcus aureus* (MRSA): Burden of disease and control challenges in Europe. *Euro. Surveill.* **15**, 19688 (2010).
36. R. H. Deurenberg, C. Vink, S. Kalenic, A. W. Friedrich, C. A. Bruggeman, E. E. Stobberingh, The molecular evolution of methicillin-resistant *Staphylococcus aureus*. *Clin. Microbiol. Infect.* **13**, 222–235 (2007).
37. D. S. Weiss, J. C. Chen, J. M. Ghigo, D. Boyd, J. Beckwith, Localization of FtsI (PBP3) to the septal ring requires its membrane anchor, the Z ring, FtsA, FtsQ, and FtsL. *J. Bacteriol.* **181**, 508–520 (1999).
38. D. J. Scheffers, L. J. Jones, J. Errington, Several distinct localization patterns for penicillin-binding proteins in *Bacillus subtilis*. *Mol. Microbiol.* **51**, 749–764 (2004).
39. K. L. Mercer, D. S. Weiss, The *Escherichia coli* cell division protein FtsW is required to recruit its cognate transpeptidase, FtsI (PBP3), to the division site. *J. Bacteriol.* **184**, 904–912 (2002).
40. T. Mohammadi, V. van Dam, R. Sijbrandi, T. Vernet, A. Zapun, A. Bouhss, M. Diepeveen-de Bruin, M. Nguyen-Distèche, B. de Kruijff, E. Breukink, Identification of FtsW as a transporter of lipid-linked cell wall precursors across the membrane. *EMBO J.* **30**, 1425–1432 (2011).
41. J. Campbell, A. K. Singh, J. P. Santa Maria Jr., Y. Kim, S. Brown, J. G. Swoboda, E. Mylonakis, B. J. Wilkinson, S. Walker, Synthetic lethal compound combinations reveal a fundamental connection between wall teichoic acid and peptidoglycan biosyntheses in *Staphylococcus aureus*. *ACS Chem. Biol.* **6**, 106–116 (2011).
42. G. Memmi, S. R. Filipe, M. G. Pinho, Z. Fu, A. Cheung, *Staphylococcus aureus* PBP4 is essential for β-lactam resistance in community-acquired methicillin-resistant strains. *Antimicrob. Agents Chemother.* **52**, 3955–3966 (2008).
43. S. R. Gill, D. E. Fouts, G. L. Archer, E. F. Mongodin, R. T. Deboy, J. Ravel, I. T. Paulsen, J. F. Kolonay, L. Brinkac, M. Beanan, R. J. Dodson, S. C. Daugherty, R. Madupu, S. V. Angiuoli, A. S. Durkin, D. H. Haft, J. Vamathevan, H. Khouri, T. Utterback, C. Lee, G. Dimitrov, L. Jiang, H. Qin, J. Weidman, K. Tran, K. Kang, I. R. Hance, K. E. Nelson, C. M. Fraser, Insights on evolution of virulence and resistance from the complete genome analysis of an early methicillin-resistant *Staphylococcus*

aureus strain and a biofilm-producing methicillin-resistant *Staphylococcus epidermidis* strain. *J. Bacteriol.* **187**, 2426–2438 (2005).
44. *Methods for Dilution Antimicrobial Susceptibility Tests for Bacteria That Grow Aerobically; Approved Standard—Seventh Edition*. *CLSI Document M7-A7* (Clinical and Laboratory Standards Institute, Wayne, PA, 2006).
45. D. Amsterdam, Susceptibility testing of antimicrobials in liquid media, in *Antibiotics in Laboratory Medicine*, V. Lorian, Ed. (Lippincott Williams & Wilkins, Philadelphia, PA, 2005), pp. 89–93.
46. A. C. Fisher, M. P. DeLisa, Laboratory evolution of fast-folding green fluorescent protein using secretory pathway quality control. *PLoS One* **3**, e2351 (2008).
47. M. Arnaud, A. Chastanet, M. Débarbouillé, New vector for efficient allelic replacement in naturally nontransformable, low-GC-content, gram-positive bacteria. *Appl. Environ. Microbiol.* **70**, 6887–6891 (2004).
48. A. M. Guérout-Fleury, K. Shazand, N. Frandsen, P. Stragier, Antibiotic-resistance cassettes for *Bacillus subtilis*. *Gene* **167**, 335–336 (1995).
49. H. Veiga, M. G. Pinho, Inactivation of the SauI type I restriction-modification system is not sufficient to generate *Staphylococcus aureus* strains capable of efficiently accepting foreign DNA. *Appl. Environ. Microbiol.* **75**, 3034–3038 (2009).
50. T. Oshida, A. Tomasz, Isolation and characterization of a Tn*551*-autolysis mutant of *Staphylococcus aureus*. *J. Bacteriol.* **174**, 4952–4959 (1992).
51. W. Kabsch, XDS. *Acta Crystallogr. D Biol. Crystallogr.* **66**, 125–132 (2010).
52. G. N. Murshudov, A. A. Vagin, E. J. Dodson, Refinement of macromolecular structures by the maximum-likelihood method. *Acta Crystallogr. D Biol. Crystallogr.* **53**, 240–255 (1997).
53. Collaborative Computational Project, Number 4, The CCP4 suite: Programs for protein crystallography. *Acta Crystallogr. D Biol. Crystallogr.* **50**, 760–763 (1994).
54. P. Emsley, B. Lohkamp, W. G. Scott, K. Cowtan, Features and development of *Coot*. *Acta Crystallogr. D Biol. Crystallogr.* **66**, 486–501 (2010).
55. V. B. Chen, W. B. Arendall III, J. J. Headd, D. A. Keedy, R. M. Immormino, G. J. Kapral, L. W. Murray, J. S. Richardson, D. C. Richardson, *MolProbity*: All-atom structure validation for macromolecular crystallography. *Acta Crystallogr. D Biol. Crystallogr.* **66**, 12–21 (2010).
56. Schrödinger, LLC, The PyMOL Molecular Graphics System.
57. S. R. Norrby, J. D. Rogers, F. Ferber, K. H. Jones, A. G. Zacchei, L. L. Weidner, J. L. Demetriades, D. A. Gravallese, J. Y. Hsieh, Disposition of radiolabeled imipenem and cilastatin in normal human volunteers. *Antimicrob. Agents Chemother.* **26**, 707–714 (1984).
58. G. L. Drusano, H. C. Standiford, C. Bustamante, A. Forrest, G. Rivera, J. Leslie, B. Tatem, D. Delaportas, R. R. MacGregor, S. C. Schimpff, Multiple-dose pharmacokinetics of imipenem-cilastatin. *Antimicrob. Agents Chemother.* **26**, 715–721 (1984).

Acknowledgments: We thank C. Boone and M. Whiteway for advice and critical reading of the manuscript. We also thank the reviewers for suggestions to improve the manuscript. **Funding:** This work is supported in part by a research grant to M.G.P. by Fundação para a Ciência e Tecnologia grants PEst-OE/EQB/LA0004/2011 and PTDC/BIA-BCM/099152/2008. P.M.P. and J.M.M. were supported by fellowships SFRH/BD/41119/2007 and SFRH/BD/71993/2010, respectively. **Author contributions:** T.R., C.M.T., A.G.T., J.L., S.H.L., and M.G.P. designed the research, interpreted the data, and wrote the manuscript. S.H.L., L.W.-J., and T.R. performed antisense screen for β-lactam susceptibility determinants. C.M.T., A.C., C.J.G., K.D., M.P., S.W., E.D., S.K., L.L., and E.M. performed mouse studies. A.G.T., C.L.-J., L.B.-P., D.C., J.V., H.W., T.C.M., and S. Sillaots performed microbiological experiments and drug resistance mapping studies. J.W., E.L., and F.L. performed pharmacokinetic studies. J.M.M., P.M.P., and M.G.P. performed fluorescence microscopy experiments. J.L., J.C.R., G.P., and S. M. Soisson performed structural biology and interpreted data. K.J.L., N.L.E., S. Sharma, K.S., and J.T. produced and purified FtsZ protein. Y.R. led synthesis of PC190723. A.B. assisted with manuscript preparation. **Competing interests:** All authors apart from J.M.M., P.M.P., A.B., and M.G.P. are or have been paid employees of Merck and may hold stock options in the company. T.R., S.H.L., and L.W.-J. have filed a patent #WO2011/112435 related to this work, "FtsZ inhibitors as potentiators of β-lactam antibiotics against methicillin resistant *Staphylococcus*." The other authors declare that they have no competing interests.

Submitted 12 December 2011
Accepted 27 February 2012
Published 21 March 2012
10.1126/scitranslmed.3003592

Citation: C. M. Tan, A. G. Therien, J. Lu, S. H. Lee, A. Caron, C. J. Gill, C. Lebeau-Jacob, L. Benton-Perdomo, J. M. Monteiro, P. M. Pereira, N. L. Elsen, J. Wu, K. Deschamps, M. Petcu, S. Wong, E. Daigneault, S. Kramer, L. Liang, E. Maxwell, D. Claveau, J. Vaillancourt, K. Skorey, J. Tam, H. Wang, T. C. Meredith, S. Sillaots, L. Wang-Jarantow, Y. Ramtohul, E. Langlois, F. Landry, J. C. Reid, G. Parthasarathy, S. Sharma, A. Baryshnikova, K. J. Lumb, M. G. Pinho, S. M. Soisson, T. Roemer, Restoring methicillin-resistant *Staphylococcus aureus* susceptibility to β-lactam antibiotics. *Sci. Transl. Med.* **4**, 126ra35 (2012).

Science Translational Medicine
AAAS

Restoring Methicillin-Resistant *Staphylococcus aureus* Susceptibility to β-Lactam Antibiotics

Christopher M. Tan, Alex G. Therien, Jun Lu, Sang H. Lee, Alexandre Caron, Charles J. Gill, Christian Lebeau-Jacob, Liliana Benton-Perdomo, João M. Monteiro, Pedro M. Pereira, Nathaniel L. Elsen, Jin Wu, Kathleen Deschamps, Mihai Petcu, Simon Wong, Etienne Daigneault, Susanne Kramer, Lianzhu Liang, Eugene Maxwell, David Claveau, John Vaillancourt, Kathryn Skorey, John Tam, Hao Wang, Timothy C. Meredith, Susan Sillaots, Lisa Wang-Jarantow, Yeeman Ramtohul, Eric Langlois, France Landry, John C. Reid, Gopal Parthasarathy, Sujata Sharma, Anastasia Baryshnikova, Kevin J. Lumb, Mariana G. Pinho, Stephen M. Soisson and Terry Roemer (March 21, 2012)
Science Translational Medicine **4** (126), 126ra35. [doi: 10.1126/scitranslmed.3003592]

Editor's Summary

A Drug Duet to Combat MRSA

Methicillin-resistant *Staphylococcus aureus* (MRSA) remains a leading cause of bloodstream infections in hospitals worldwide. MRSA infection rates in the United States reported as recently as 2005 estimate that mortality associated with MRSA exceeded that of HIV/AIDS in the same year. Compounding this issue is the rapid emergence of community-acquired MRSA infections in healthy individuals and the difficulty within the pharmaceutical industry regarding discovery of new and efficacious single-agent antibiotics to treat bacterial pathogens resistant to traditional antibiotics. MRSA drug resistance is attributed to the acquisition of an accessory penicillin-binding protein (PBP2A), which is refractory to the inhibitory activity of penicillin and other β-lactam antibiotics. To thwart this resistance mechanism, Tan *et al*. sought to identify alternative drug targets that, when inhibited by genetic means, resensitized MRSA to β-lactam antibiotics. They discovered that a target class displaying this phenotype in *S. aureus* comprised proteins involved in cell division including FtsZ, the bacterial ancestor of tubulin. The researchers then demonstrated that the FtsZ-specific inhibitor PC190723 acts synergistically with β-lactam antibiotics in vitro and in vivo and that this combination was efficacious in a mouse model of MRSA infection. Fluorescence microscopy localization studies revealed that the chemical synergy between these agents is likely to be elicited by the concomitant delocalization of their drug targets: FtsZ and PBP2. Next, the authors resolved a 2.0 Å crystal structure of *S. aureus* FtsZ in complex with PC190723 and identified mutations in FtsZ that confer resistance against PC190723 on MRSA. However, combining PC190723 with a β-lactam antibiotic markedly reduced the spontaneous frequency with which PC190723 drug resistance mutations emerged in MRSA. Moreover, MRSA with PC190723 resistance mutations displayed attenuated virulence and restored susceptibility to β-lactam antibiotics. Together, these data support a target-based approach to develop synergistic drug combinations to combat MRSA with improved efficacy and reduced potential for drug resistance.